

# The classification of BL Lacertae objects: the Ca H&K break

Hermine Landt<sup>1,2</sup>, Paolo Padovani<sup>1,3,4</sup>, Paolo Giommi<sup>5</sup>

<sup>1</sup> *Space Telescope Science Institute, 3700 San Martin Drive, Baltimore, MD 21218, USA*

<sup>2</sup> *Hamburger Sternwarte, Gojenbergsweg 112, D-21029 Hamburg, Germany*

<sup>3</sup> *Affiliated to the Astrophysics Division, Space Science Department, European Space Agency*

<sup>4</sup> *On leave from Dipartimento di Fisica, II Università di Roma “Tor Vergata”, Via della Ricerca Scientifica 1, I-00133 Roma, Italy*

<sup>5</sup> *ASI Science Data Center, c/o ESRIN, Via G. Galilei, I-00044 Frascati, Italy*

Accepted , Received

## ABSTRACT

We investigate why BL Lacertae objects (BL Lacs) have values of the Ca H&K break (a stellar absorption feature) lower than low-power radio galaxies and if its use is justified to separate the two classes. For this purpose we relate this parameter to the radio and optical core emissions, as well as to the X-ray powers, for a sample of  $\sim 90$  radio sources. We find that the Ca H&K break value decreases with increasing jet powers, and that it also anti-correlates with the radio core dominance parameter but not with extended radio emission. Based on this we conclude that the Ca H&K break value of BL Lacs and radio galaxies is a suitable indicator of orientation. From the luminosity ratios between objects with low and high Ca H&K break values we constrain the average Lorentz factors for BL Lacs and low-power radio galaxies in the radio and X-ray band to  $\Gamma \sim 2 - 4$  and derive average viewing angles for the galaxies. Our values are in agreement with results from independent methods. We find that the correlations between Ca H&K break and radio core and X-ray luminosity hold independently for low- (LBL) and high-energy peaked BL Lacs (HBL). We derive average viewing angles for their parent populations, which turn out to be similar to the ones for our entire sample, and compare for the first time the luminosities of LBL and HBL at different orientations.

**Key words:** BL Lacertae objects: general

## 1 INTRODUCTION

BL Lacertae objects (BL Lacs) are set apart from other types of active galactic nuclei by their extreme properties, namely, irregular, rapid variability, strong optical and radio polarization, core-dominant radio morphology, and a broad continuum extending from the radio through the  $\gamma$ -rays. These properties are believed to be due to the fact that BL Lacs are low-luminosity radio galaxies (Fanaroff-Riley type I [FR I]; Fanaroff & Riley 1974) whose jets are aligned close to the observer’s line of sight (first proposed by Blandford & Rees 1978). At such small viewing angles, relativistic effects cause the jet’s luminosity to appear amplified, and therefore we refer to BL Lacs as “beamed” FR I radio galaxies.

The classification of an active galactic nucleus (AGN) as a BL Lac has been controversial ever since the first sur-

veys which included a sizeable number of these objects, and has somewhat varied over time. Two of the early surveys to select a large number of BL Lacs were the 1 Jy in the radio (Stickel et al. 1991; Rector & Stocke 2001) and the *EINSTEIN* Medium Sensitivity Survey (EMSS) in the X-ray band (Stocke et al. 1991; Morris et al. 1991). The 1 Jy radio survey used two criteria to classify an object as a BL Lac: a flat radio spectrum ( $\alpha_r \leq 0.5$ , where  $S_\nu \propto \nu^{-\alpha}$ ) and an optical spectrum with emission lines weaker than 5 Å rest-frame equivalent width. This latter criterion was chosen to separate BL Lacs from their more powerful siblings, the flat spectrum radio quasars (FSRQ). Other BL Lac properties, such as strong polarization and rapid variability, were not regarded as necessary requirements. Nevertheless, optical polarization studies, available at the time, gave values above 3% for almost all objects (Kühr & Schmidt 1990),

and their strong and irregular variability was quantified later by Heidt & Wagner (1996).

The EMSS X-ray survey, on the other hand, did not use any radio information to classify its objects (allowing for the existence of radio-quiet X-ray emitting BL Lacs, which could not be found), but introduced a limit on the Ca H&K break value as an additional criterion. The Ca H&K break, also referred to as “Ca II break” or “contrast”, is a stellar absorption feature typically found in the spectra of elliptical galaxies. Its value in non-active elliptical galaxies is on average  $\sim 50\%$  (Dressler & Shectman 1987). Stocke et al. (1991) chose a limiting value of 25% for the EMSS BL Lacs in order to ensure the presence of a substantial non-thermal jet continuum in addition to the thermal spectrum of the host galaxy. As regards polarization (Stocke et al. 1991; see also Jannuzi et al. 1994) and variability (Heidt & Wagner 1998) data, EMSS BL Lacs were found to have somewhat lower values than the ones typical of 1 Jy BL Lacs. However, similarly to the 1 Jy survey, these two BL Lac properties were not used as part of the classification scheme.

The two defining criteria for a BL Lac used by the EMSS, a diluted Ca H&K break and no or very weak emission lines in the optical spectrum, were revised by Marchã et al. (1996). In order to additionally include in surveys radio sources with a strong host galaxy contribution which might hide weak BL Lacs, these authors proposed to expand the limit on the Ca H&K break up to a value of 40% and accordingly, due to a lower continuum in these objects, the allowed rest frame equivalent width of the strongest emission line up to a value of  $\sim 50$  Å. In fact, they suggested a triangular region in the contrast, equivalent width plane (see their Fig. 6) to be used to separate BL Lacs both from radio galaxies and quasars. BL Lacs selected according to these extended criteria were termed “BL Lac candidates”, in order to distinguish them from those fulfilling the classical criteria. Recent surveys, like RGB (Laurent-Muehleisen et al. 1998), DXRBS (Perlman et al. 1998; Landt et al. 2001), the Sedentary Survey (Giommi, Menna & Padovani 1999), and REX (Caccianiga et al. 1999, 2000), employ this revised version of the BL Lac classification.

In this paper, we investigate why BL Lacs have lower Ca H&K break values than low-power radio galaxies. In Section 2, we relate the Ca H&K break value to optical jet power. In Section 3, we expand our studies to the radio and X-ray band. In Section 4, we determine a possible relation between Ca H&K break value and viewing angle. An application of our studies to the two BL Lac subclasses, low- and high-energy peaked BL Lacs, is presented in Section 5. Finally, in Section 6, we discuss our results and present our conclusions. Throughout this paper, we assumed the following cosmological parameters,  $H_0 = 50$  km/s/Mpc and  $q_0 = 0$ .

## 2 THE OPTICAL BL LAC CONTINUUM

According to current unified schemes for radio-loud AGN, BL Lacs are beamed FR I radio galaxies. Therefore, in their optical spectra we see the amplified non-thermal emission from the jet in addition to thermal emission from the underlying host galaxy, normally a luminous elliptical

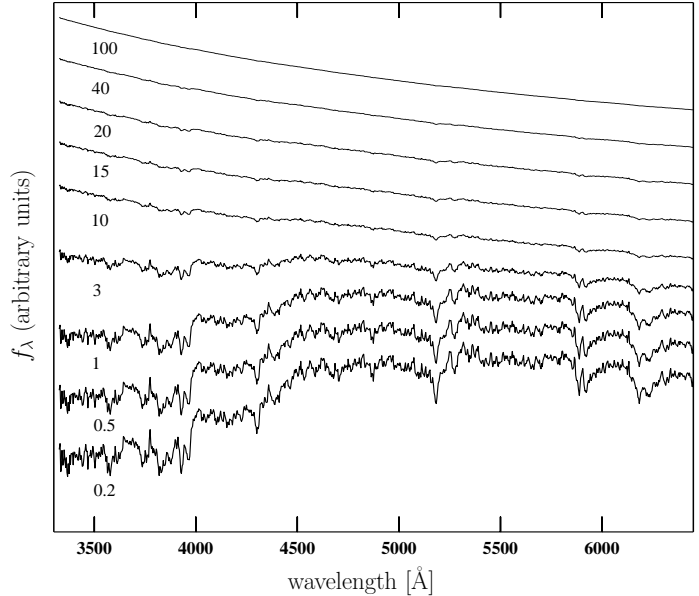


**Figure 1.** Simulated BL Lac spectra  $f_\lambda$  vs.  $\lambda$  for a jet of optical spectral slope  $\alpha_\lambda = \alpha_\nu = 1$  and of increasing flux relative to the underlying host galaxy. The assumed jet/galaxy ratios (defined at 5500 Å) are from bottom to top: 0.2, 0.5, 1, 3, 10, 15, 20, 40, and 100.

(e.g., Wurtz, Stocke & Yee 1996). The non-thermal and thermal components have different shapes, and their relative strengths determine the observed BL Lac continuum. The jet component can be locally best described by a single power law of the form  $S_\nu \propto \nu^{-\alpha_\nu}$  (or equivalently  $S_\lambda \propto \lambda^{-\alpha_\lambda}$ , where  $\alpha_\lambda = 2 - \alpha_\nu$ ). The spectrum of the host galaxy, on the other hand, has an approximate black body shape and contains absorption features typical of ellipticals.

For our studies we have simulated possible BL Lac continua. For this purpose, we assumed the jet overlaying the elliptical host galaxy to vary in intensity and optical spectral slope. We used values between 0.2 and 100 for the jet/galaxy ratio (defined at 5500 Å), and assumed for the optical spectral slope the three cases  $\alpha_\nu = 0, 1, 2$ , following the results of Falomo, Scarpa & Bersanelli (1994), and included additionally the extreme case of  $\alpha_\nu = 4$ .

Fig. 1 shows the resulting simulated BL Lac spectra representatively for a jet of optical spectral slope  $\alpha_\lambda = \alpha_\nu = 1$ . As the jet steadily increases relative to the galaxy, two effects are visible. The shape of the BL Lac continuum resembles more and more a power-law spectrum and the galactic absorption features become weaker. One prominent absorption feature typically seen in the spectra of elliptical galaxies is the Ca H&K break located at  $\sim 4000$  Å rest frame wavelength. This feature, also referred to as “Ca II break” or “contrast”, is defined as  $C = (f_+ - f_-)/f_+$ , where  $f_-$  and  $f_+$  are the fluxes in the rest frame wavelength regions 3750 – 3950 Å and 4050 – 4250 Å respectively. Its value in normal non-active elliptical galaxies is found to be on average  $\sim 0.5$  (Dressler & Shectman 1987). In BL Lacs, the value of the Ca H&K break is decreased by the non-thermal jet

emission. We note that the Ca H&K break value is related to the discontinuity at 4000 Å [D(4000); Bruzual 1983] by  $C = 1 - 1/D(4000)$ , and is measured in spectra plotted as  $f_\nu$  versus  $\nu$ . However, if measured in spectra plotted as  $f_\lambda$  versus  $\lambda$ , the relation  $C_\nu = 0.14 + 0.86 \cdot C_\lambda$  can be used to convert one to the other.

In order to quantify how the amplified jet emission changes the Ca H&K break value, we measured this feature in each of our simulated spectra. In the case where the jet dominates the object’s spectrum, we set the Ca H&K break value equal to zero (its minimum possible value in our simulations). For every case of  $\alpha_\nu$ , we get that there is a significant ( $P > 99.99\%$ ) linear anti-correlation between the assumed jet/galaxy ratio and the Ca H&K break value (dotted lines in Fig. 2).

To assess how well this result is reproduced by observations we need information on Ca H&K break value and jet/galaxy ratios for a sizeable sample of BL Lacs. Observational jet/galaxy ratios were obtained from the imaging studies of Urry et al. (2000) which allow the separation of the core flux from that of the host galaxy. These authors used the HST Wide Field Planetary Camera 2 (WFPC 2) to image in snapshot mode a sample of 132 BL Lacs from different radio and X-ray surveys. Most of their images were taken in the F702W filter (similar to Cousin R filter), but those already observed in F814W during an earlier HST cycle were reobserved in F606W (a filter similar to Johnson V). We derived jet/galaxy ratios at 5500 Å by converting  $R$  magnitudes to  $V$  magnitudes. We assumed  $V - R = 0.3$  for the core component (Urry et al. 2000), while for the host galaxy magnitudes we used the redshift-dependent  $V - R$  values as tabulated by Urry et al. (2000; see their Table 2). Ca H&K break values for 48 of these sources were derived from the literature and also from our own measurements (see Sect. 3).

For these BL Lacs, we plot in Fig. 2 the jet/galaxy ratio vs. Ca H&K break value. An analysis using the ASURV package (Feigelson & Nelson 1985), that allows us to include upper limits, shows that these two quantities are significantly ( $P > 99.99\%$ ) anti-correlated, in agreement with our simulations. Furthermore, a partial correlation analysis shows that this correlation is not induced by a common redshift dependence. In Fig. 2 we plot the observed correlation between optical jet/galaxy ratio and Ca H&K break value (solid line) in addition to the correlations obtained from our simulations (dotted lines). A comparison between the two indicates that the scatter in the observed correlation ( $\sim 0.6$ ) is likely induced by jets of different optical spectral slopes.

We have shown using both simulations and observational data that the Ca H&K break value in BL Lacs anti-correlates with optical jet/galaxy ratio. At this point the question arises if this correlation could possibly mask a correlation between jet emission and Ca H&K break value or between host galaxy emission and Ca H&K break value. Urry et al. (2000) find that the distribution of the absolute magnitudes of BL Lac host galaxies has a relatively small dispersion  $\Delta M_R = 0.6$  mag. This result is based on detected host galaxies of a very large number of BL Lacs (72 sources) covering the redshift range  $0.024 \leq z \leq 0.7$ .

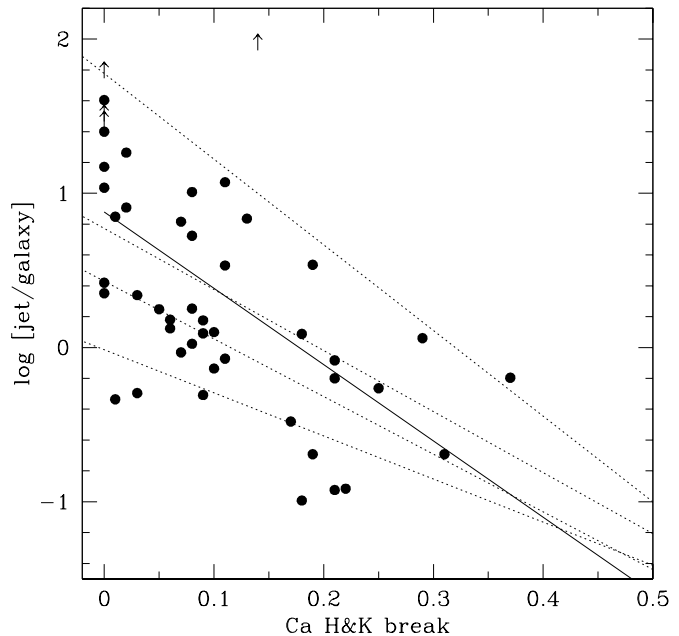


**Figure 2.** The jet/galaxy flux ratio (at 5500 Å) vs. the Ca H&K break value for BL Lacs from Urry et al. (2000). Arrows indicate lower limits on the jet/galaxy ratio. The solid line represents the observed correlation. Dotted lines represent the correlations obtained from our simulations for optical spectral slopes  $\alpha_\nu = 0, 1, 2, 4$  (from bottom to top).

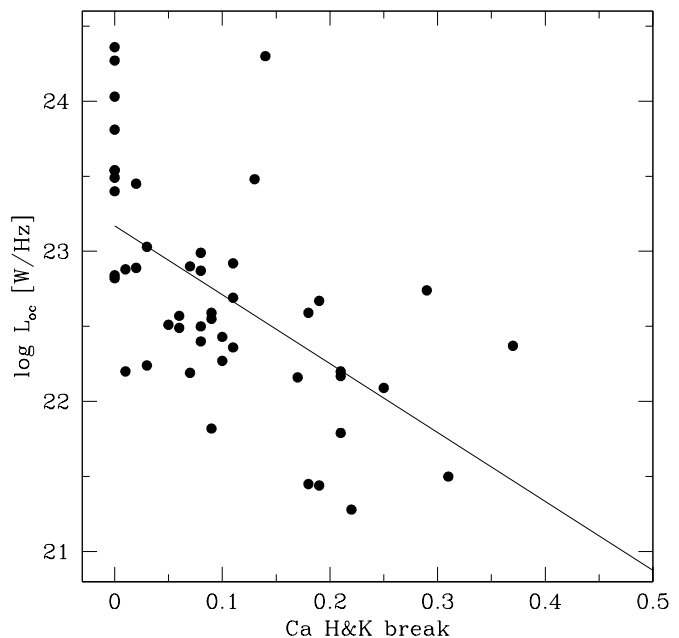


**Figure 3.** The optical core luminosity vs. the Ca H&K break value for BL Lacs from Urry et al. (2000). The solid line represents the observed correlation.

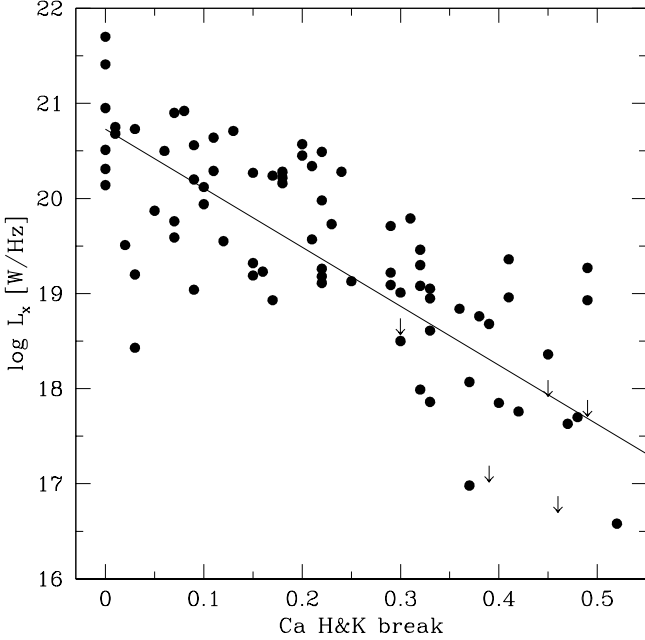


**Figure 4.** The 1 keV X-ray luminosity vs. the Ca H&K break value. Arrows denote upper limits. The solid line represents the observed correlation. Object 1241+735 is off the plot.

The relatively small dispersion found by Urry et al. (2000) implies that the luminosity of BL Lac host galaxies can be regarded as roughly constant. Therefore, the observed increase in jet/galaxy ratio (with decreasing Ca H&K break) can be related directly to an increase in jet power. Indeed, for our sample of objects we find that, on one hand, the optical core luminosity (from Urry et al. 2000) is significantly ( $P > 99.9\%$ ) anti-correlated with the Ca H&K break value (see Fig. 3), and that, on the other hand, no significant ( $P = 88\%$ ) correlation is present between host galaxy luminosity and Ca H&K break value.

### 3 FROM A BL LAC TO A RADIO GALAXY

In the previous section, we have shown that the Ca H&K break value in BL Lacs is decreased due to an increase in optical jet power. Here we want to investigate this further by relating the Ca H&K break value also to the radio and X-ray properties of both BL Lacs and FR I radio galaxies.

We have then collected from the literature and from our own data information on the Ca H&K break value, ROSAT X-ray band (0.1 – 2.4 keV) flux, total radio flux at 1.4 (NVSS) and 5 GHz, and core radio flux. From these we have computed the luminosities, radio core dominance parameter and radio spectral index  $\alpha_r$  which are listed in Table 1 (see footnotes to Table 1 for details). We also give in Table 1 the references for the Ca H&K break value, and the radio core and X-ray fluxes. The radio core flux measurements are largely based on observations with the Very Large Array (VLA). The total radio flux at 5 GHz was obtained from the

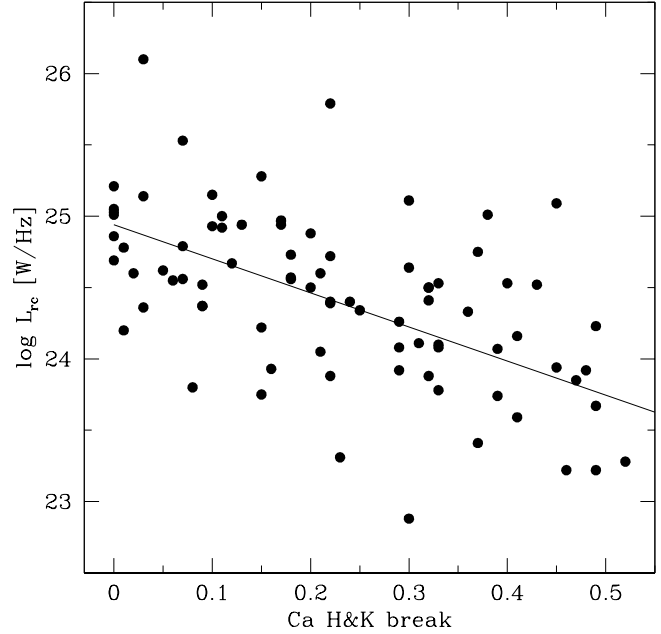


**Figure 5.** The radio core luminosity at 5 GHz vs. the Ca H&K break value. The solid line represents the observed correlation.

GB6 survey (Gregory et al. 1996), with the following exceptions: for the 1 and 2 Jy objects we used the values given in Stickel et al. (1994) and Wall & Peacock (1985), for the EMSS objects we used the measurements given in Stocke et al. (1991), for Slew objects not detected in the GB6 we used the values given in Perlman et al. (1996b), and for southern DXRBS sources we give the total radio flux at 5 GHz from the PMN survey (Griffith & Wright 1993).

The BL Lacs and FR I radio galaxies were selected from the following surveys: 1 Jy survey (Stickel, Meisenheimer & Kühr 1994), 2 Jy survey (Tadhunter et al. 1993), 200 mJy sample (Marchã et al. 1996), EMSS (Rector, Stocke & Perlman 1999, 2000), Slew survey (Perlman et al. 1996b), RGB (Laurent-Muehleisen et al. 1998), and DXRBS (Perlman et al. 1998; Landt et al. 2001). From these surveys we chose in fact all objects with a rest frame equivalent width of the strongest emission line  $< 60 \text{ \AA}$ , an available Ca H&K break value, and *both* a radio core and X-ray flux measurement. We required available fluxes in both radio and X-ray band in order to avoid comparing two different sets of objects in the luminosity - Ca H&K break plane (see Sect. 3.1). However, while for a particular object it is always possible to obtain an upper limit on its ROSAT X-ray luminosity from the exposure maps of the RASS (Voges et al. 1999), this is not the case for its radio core luminosity and the object will not be included in our sample. The limit on the emission line strength is based on the results of Marchã et al. (1996, see their Fig. 6) and was chosen to exclude flat spectrum radio quasars. An exclusion of objects whose power is typical of FR II radio galaxies can be based on the value of the extended radio emission. Following the results of Owen & Ledlow (1994), we chose a value of  $L_{\text{ext}} = 10^{25.6} \text{ W/Hz}$

Table 1. BL Lacs and FR I radio galaxies

Survey	Name	z	C	$\sigma$	Ref. C	log $L_x$ 1 keV [W/Hz]	Ref. $f_x$	log $L_{rc}$ 5 GHz [W/Hz]	Ref. $f_{rc}$	Radio Array	log $L_{ext}$ 5 GHz [W/Hz]	log R 5 GHz	$\alpha_r$
(1)	(2)	(3)	(4)	(5)	(6)	(7)	(8)	(9)	(10)	(11)	(12)	(13)	(14)
1 Jy	0118–272	0.559	0.00	0.02	v	20.45	a	26.94	m	IV	26.81	0.13	–0.16
1 Jy	0138–097	0.733	0.00	0.03	v	20.56	a	27.12	m	IV	26.99	0.13	–0.50
1 Jy	0218+357	0.685	0.12	0.09	v	< 20.51	A	27.25	o	XI	27.07	0.18	0.31
1 Jy	0828+493	0.548	0.08	0.06	v	< 20.29	A	26.55	y	II	26.78	–0.23	–0.88
1 Jy	1538+149	0.605	0.00	0.03	v	20.77	x	27.13	y	II	27.19	–0.06	–0.28
1 Jy	1823+568	0.664	0.02	0.03	v	21.02	x	27.05	y	II	27.31	–0.26	–0.13
2 Jy	0625–53	0.054	0.15	0.12	v	19.32	b	23.75	p	IX	25.37	–1.62	1.06
2 Jy	0915–11	0.054	0.36	0.01	w	19.84	b	24.45	p	VII	26.24	–1.79	0.82
200 mJy	0055+300	0.015	0.46		u	< 16.87	A	23.22	n	X	22.93	0.29	0.90
200 mJy	0116+319	0.060	0.45		u	< 18.09	A	25.09	n	X	25.11	–0.02	0.42
200 mJy	0149+710	0.022	0.33		u	17.86	c	23.78	q	III	23.87	–0.09	–0.10
200 mJy	0210+515	0.049	0.15		u	19.19	c	24.22	q	III	24.09	0.13	0.04
200 mJy	0651+410	0.021	0.39		u	< 17.19	A	23.74	o	IV	23.39	0.35	–0.51
200 mJy	0651+428	0.126	0.17		u	18.93	c	24.97	q	III	24.55	0.42	0.06
200 mJy	0733+597	0.041	0.49		u	< 17.88	A	24.23	q	III	23.97	0.26	0.36
200 mJy	1055+567	0.410	$\leq 0.05$		u	20.77	c	26.11	q	III	25.76	0.35	–0.10
200 mJy	1101+384	0.031	0.24		u	20.28	d	24.40	q	VIII	23.71	0.69	0.05
200 mJy	1133+704	0.046	0.31		u	19.79	d	24.11	q	III	24.09	0.02	0.15
200 mJy	1144+352	0.063	0.37		u	18.07	d	24.75	q	III	24.75	0.00	–0.03
200 mJy	1217+295	0.002	0.42		u	17.76	A	21.69	q	VIII	20.86	0.83	0.13
200 mJy	1241+735	0.075	0.43		u	< 15.00	A	24.52	n	X	24.70	–0.18	–0.13
200 mJy	1418+546	0.151	0.03		u	19.20	d	26.10	q	VIII	25.46	0.64	–0.62
200 mJy	1652+398	0.031	0.07		u	19.59	d	24.79	m	IV	23.46	1.33	0.10
200 mJy	1744+260	0.147	$\leq 0.3$		u	< 18.74	A	25.11	n	X	25.09	0.02	0.23
200 mJy	1807+698	0.046	0.03		u	18.43	d	25.14	m	IV	24.79	0.35	–0.12
200 mJy	2320+203	0.038	0.47		u	17.63	d	23.85	q	III	24.18	–0.33	0.03
EMSS	MS0011.7+0837	0.162	0.30	0.04	e	19.01	e	24.64	e	II	24.80	–0.16	1.13
EMSS	MS0122.1+0903	0.338	0.22	0.18	s	19.18	f	23.88	s	II	< 23.74	> 0.14	
EMSS	MS0158.5+0019	0.298	0.09	0.02	s	20.56	f	24.37	z	II	24.35	0.02	0.13
EMSS	MS0257.9+3429	0.246	0.25	0.06	s	19.13	f	24.34	z	II	23.70	0.64	0.10
EMSS	MS0317.0+1834	0.190	0.21	0.06	s	19.57	f	24.05	z	II	24.21	–0.16	0.24
EMSS	MS0419.3+1943	0.516	0.11	0.07	s	20.64	f	24.92	s	II	24.23	0.69	0.09
EMSS	MS0607.9+7108	0.267	0.09	0.04	s	19.04	f	24.52	z	II	24.43	0.09	0.31
EMSS	MS0737.9+7441	0.314	0.00	0.01	s	20.51	f	24.86	z	II	24.48	0.38	–0.02
EMSS	MS0922.9+7459	0.638	0.20	0.07	s	20.57	f	24.88	s	II	< 24.03	> 0.85	
EMSS	MS1019.0+5139	0.141	0.23	0.05	s	19.73	e	23.31	s	V	22.29	1.02	0.61
EMSS	MS1050.7+4946	0.140	0.32	0.07	s	19.46	e	24.50	s	V	24.18	0.32	0.15
EMSS	MS1154.1+4255	0.172	0.33	0.10	s	18.95	e	24.08	e	V	23.17	0.91	0.57
EMSS	MS1207.9+3945	0.616	0.07	0.04	s	20.90	f	25.53	s	V	24.59	0.94	0.95
EMSS	MS1209.0+3917	0.602	0.15	0.13	s	20.27	e	25.28	e	V	< 24.31	> 0.97	0.67
EMSS	MS1221.8+2452	0.218	0.02	0.02	s	19.51	f	24.60	z	II	24.14	0.46	–0.02
EMSS	MS1229.2+6430	0.164	0.18	0.09	s	20.16	f	24.56	z	II	24.18	0.38	0.27
EMSS	MS1235.4+6315	0.297	0.05	0.07	s	19.87	f	24.62	s	V	< 23.24	> 1.38	0.47
EMSS	MS1407.9+5954	0.496	0.10	0.05	s	20.12	f	25.15	z	II	24.97	0.18	0.64
EMSS	MS1443.5+6349	0.298	0.22	0.06	s	19.98	f	24.40	z	II	24.40	0.00	0.39
EMSS	MS1458.8+2249	0.235	0.00	0.01	s	20.14	f	24.69	z	II	24.37	0.32	0.07
EMSS	MS1534.2+0148	0.311	0.11	0.06	s	20.29	f	25.00	z	II	24.84	0.16	0.61
EMSS	MS1552.1+2020	0.273	0.13	0.09	s	20.71	f	24.94	z	II	24.73	0.21	0.60
EMSS	MS1757.7+7034	0.406	0.01	0.00	s	20.68	f	24.78	s	II	< 24.27	> 0.51	
EMSS	MS2143.4+0704	0.235	0.10		j	19.94	f	24.93	z	II	24.70	0.23	0.57
EMSS	MS2347.4+1924	0.515	0.18	0.16	s	20.28	s	24.57	s	II	23.88	0.69	0.36
SLEW	1ES0120+340	0.272	0.00	0.04	v	21.41	h	25.03	r	VI	24.01	1.02	0.24
SLEW	1ES0229+200	0.139	0.21	0.07	v	20.34	g	24.60	r	VI	22.97	1.63	0.48
SLEW	1ES0502+675	0.416*	0.00	0.04	v	21.70	h	25.21	q	I	24.52	0.69	0.04
SLEW	1ES0806+524	0.138	0.00	0.04	v	20.31	h	25.01	q	III	24.63	0.38	0.03
SLEW	1ES0927+500	0.188	0.03	0.07	v	20.73	i	24.36	q	III	24.04	0.32	–0.02
SLEW	1ES1255+244	0.140	0.08	0.11	v	20.92	r	23.80	r	VI	22.65	1.15	0.55
SLEW	1ES1426+428	0.129	0.01		j	20.75	h	24.20	q	I	24.09	0.32	0.35
SLEW	1ES1440+122	0.162	0.18		j	20.22	h	24.73	q	VIII	23.71	1.02	0.26

**Table 1** – *continued*

Survey	Name	z	C	$\sigma$	Ref. C	log $L_x$ 1 keV [W/Hz]	Ref. $f_x$	log $L_{rc}$ 5 GHz [W/Hz]	Ref. $f_{rc}$	Radio Array	log $L_{ext}$ 5 GHz [W/Hz]	log R 5 GHz	$\alpha_r$
(1)	(2)	(3)	(4)	(5)	(6)	(7)	(8)	(9)	(10)	(11)	(12)	(13)	(14)
SLEW	1ES1741+196	0.083	0.12	0.05	v	19.55	h	24.67	q	III	24.73	-0.06	-0.07
SLEW	1ES1853+671	0.212	0.09	0.05	v	20.20	r	24.37	r	VI	< 22.87	> 1.50	-0.07
SLEW	1ES2326+174	0.213	0.06	0.05	v	20.50	r	24.55	r	VI	24.23	0.32	-0.03
RGB	RGBJ0110+418	0.096	0.32		j	19.08	j	23.88	q	I	23.88	0.00	0.70
RGB	RGBJ0152+017	0.080	0.29		j	19.22	j	24.26	q	VIII			0.12
RGB	RGBJ0314+247	0.054	0.30		j	18.50	j	22.88	q	VIII	23.65	-0.77	-1.16
RGB	RGBJ0656+426	0.059	0.36		j	18.84	j	24.33	q	III	24.72	-0.39	0.53
RGB	RGBJ0710+591	0.125	0.22		j	20.49	j	24.39	q	I	24.54	-0.15	0.54
RGB	RGBJ0806+728	0.098	0.16		j	19.23	j	23.93	q	I	23.67	0.26	0.39
RGB	RGBJ0820+488	0.130	0.41		j	18.96	j	23.59	q	I	24.84	-1.25	0.59
RGB	RGBJ1136+676	0.136	0.20		j	20.45	j	24.50	q	I	23.81	0.69	-0.04
RGB	RGBJ1253+509	0.121	0.49		j	18.93	j	23.67	q	I	24.33	-0.66	0.51
RGB	RGBJ1324+576	0.115	0.41		j	19.36	j	24.16	q	I	23.98	0.18	0.04
RGB	RGBJ1417+257	0.237	0.00		j	20.95	j	25.05	q	VIII			0.67
RGB	RGBJ1427+541	0.105	0.39		j	18.68	j	24.07	q	VI	23.65	0.42	0.24
RGB	RGBJ1516+293	0.130	0.32		j	19.30	j	24.41	q	I			
RGB	RGBJ1532+302	0.064	0.29		j	19.09	j	23.92	q	III	23.16	0.76	-0.01
RGB	RGBJ1745+398	0.267	0.17		j	19.86	j	25.64	q	III	25.70	-0.06	0.75
RGB	RGBJ1750+470	0.160	0.29		j	19.71	j	24.08	q	I	24.66	-0.58	0.59
RGB	RGBJ1823+334	0.108	0.49		j	19.27	j	23.22	q	I	24.50	-1.28	0.91
RGB	RGBJ1841+591	0.530	0.17		j	20.24	j	24.94	q	I			
RGB	RGBJ2241+048	0.069	0.45		j	18.36	j	23.94	q	III	24.14	-0.20	0.42
RGB	RGBJ2250+384	0.119	0.07		j	19.76	j	24.56	q	III	24.56	0.00	-0.11
RGB	RGBJ2322+346	0.098	0.33		j	19.05	j	24.10	q	I	24.30	-0.20	0.17
RGB	RGBJ2323+205	0.041	0.48		j	17.70	j	23.92	q	III	24.25	-0.33	0.03
DXRBS	WGAJ0032.5-2849	0.324	0.22	0.08	k	19.11	k	25.79	t	IX	24.88	0.91	0.08
DXRBS	WGAJ0340.8-1814	0.195	0.40	0.08	k	17.85	k	24.53	t	IX	25.37	-0.84	0.57
DXRBS	WGAJ0428.8-3805	0.150	0.32	0.05	k	17.99	k	24.50	t	IX	24.24	0.26	-0.03
DXRBS	WGAJ0528.5-5820	0.254	0.38	0.18	l	18.76	k	25.01	t	IX	25.29	-0.28	0.46
DXRBS	WGAJ0624.7-3230	0.252	0.22	0.05	k	19.26	k	24.72	t	IX	25.29	-0.47	-0.54
DXRBS	WGAJ0816.0-0736	0.040	0.37	0.18	k	16.98	k	23.41	t	IX	23.20	0.21	-0.28
DXRBS	WGAJ1057.6-7724	0.181	0.48	0.18	l	18.14	k	25.38	t	IX	25.66	-0.28	0.71
DXRBS	WGAJ1311.3-0521	0.160	0.33	0.12	l	18.61	l	24.53	t	IX	24.30	0.23	0.37
DXRBS	WGAJ1457.9-2124	0.319	0.45	0.20	l	19.57	l	25.25	t	IX	25.80	-0.55	0.79
DXRBS	WGAJ2317.4-4213	0.056	0.52	0.08	k	16.58	k	23.28	t	IX	24.22	-0.94	0.53

columns: (1) survey, (2) object name, (3) redshift, (4) Ca H&K break value (measured in spectra  $f_\lambda$  vs.  $\lambda$ ), (5)  $1\sigma$  error on the Ca H&K break value, (6) reference for Ca H&K break measurement, (7) X-ray luminosity at 1 keV (ROSAT X-ray band (0.1 - 2.4 keV) flux transformed to 1 keV and luminosity k-corrected assuming spectral index  $\alpha_x = 1.2$ ), (8) reference for ROSAT X-ray band flux, (9) radio core luminosity at 5 GHz (transformed to 5 GHz and k-corrected assuming  $\alpha_r$  from column (14) or else  $\alpha_r = 0.3$ ), (10) reference for radio core flux, (11) radio array used for observations of radio core flux (see below), (12) extended radio luminosity at 5 GHz, (13) radio core dominance, (14) radio spectral index between 1.4 (NVSS) and 5 GHz (computed from the object's total fluxes)

radio array: (I) VLA A at 5 GHz, (II) VLA A at 1.5 GHz, (III) VLA BnA at 5 GHz, (IV) VLA B at 5 GHz, (V) VLA B at 1.5 GHz, (VI) VLA CnB at 5 GHz, (VII) VLA C at 5 GHz, (VIII) VLA D at 5 GHz, (IX) ATCA at 5 GHz, (X) MERLIN at 5 GHz, (XI) VLBI at 1.5 GHz

references: (a) Siebert et al. 1998, (b) Brinkmann, Siebert & Boller 1994, (c) Brinkmann et al. 1997, (d) Brinkmann et al. 1995, (e) Rector, Stocke & Perlman 1999, (f) Perlman et al. 1996a, (g) Nass et al. 1996, (h) Laurent-Muehleisen et al. 1999, (i) Bade et al. 1998, (j) Laurent-Muehleisen et al. 1998, (k) Perlman et al. 1998, (l) Landt et al. 2001, (m) Cassaro et al. 1999, (n) Augusto, Wilkinson & Browne 1998, (o) Taylor et al. 1996, (p) Morganti, Killeen & Tadhunter 1993, (q) Laurent-Muehleisen et al. 1997, (r) Perlman et al. 1996b, (s) Rector et al. 2000, (t) from ATCA observations of the DXRBS, (u) Marchā et al. 1996, (v) measured on spectrum, (w) Owen, Ledlow & Keel 1996, (x) RASS/NVSS-ASDC catalogue (Giommi et al. in prep.), (y) Murphy, Browne & Perley 1993, (z) Perlman & Stocke 1993, (A) ROSAT All Sky Survey (Voges et al. 1999); upper limit estimated from exposure maps

\* we obtained this redshift, which is different from the one published by Perlman et al. (1996b), after a careful reinspection of the electronic spectral file

(transformed from 1400 MHz using a radio spectral index  $\alpha_r = 0.8$ ) to separate the less luminous FR I radio galaxies from the more luminous FR II radio galaxies. These authors find that basically only FR II radio galaxies have an extended radio emission above this value. The extended radio power was computed as  $L_{\text{ext}} = L_{\text{tot}} - L_{\text{rc}}$ , where  $L_{\text{tot}}$  and  $L_{\text{rc}}$  are the object's total and core radio powers at 5 GHz respectively. We note that we *assume* that our low-power radio galaxies are FR Is, although we do not have any information on their radio morphology. Bondi et al. (2001) have indeed shown that the nuclear properties of the weak-lined radio galaxies in the 200 mJy sample are consistent with those of FR Is, although their radio morphology might not be consistent in all cases with an FR I classification. Our sample comprises 83 objects. However, in Table 1 we additionally list 7 objects that meet the current classification criteria for a BL Lac but have extended radio powers typical of FR II radio galaxies. We will use these sources only for our comparison studies in Sect. 5.2.

We measured the Ca H&K break values for objects from the 1 Jy, 2 Jy, Slew survey, and DXRBS on the reduced and calibrated spectra. For sources from the 200 mJy sample, EMSS, and RGB, we used the Ca H&K break values listed in the literature. We note that we excluded from our study sources with errors on the Ca H&K break value  $> 0.2$ . The error on the Ca H&K break listed in Table 1 represents the  $1 \sigma$  limit and was computed based on the signal-to-noise ratio (SNR) blueward and redward of the feature. The error is on average 0.07 for the sources included in our study. No errors were available for sources from the 200 mJy sample and RGB. Nevertheless, the spectra of the RGB objects are quoted to have a SNR  $\gtrsim 30$  (Laurent-Muehleisen et al. 1998) and therefore the error on the Ca H&K break value for these sources is expected to be small.

Our sample is highly heterogeneous, being a collection of surveys with different selection bands and flux limits. However, similarly to the studies of Padovani & Giommi (1996), this approach offers us the possibility to maximize the coverage of the parameter space and therefore to look for correlations in a way which would not be possible by considering individual samples separately. This approach is acceptable whenever the parameter values or correlations studied are not strongly influenced by the sample selection.

### 3.1 The radio core and X-ray luminosity

In the optical band, the spectrum of a BL Lac is made up of two components, a thermal (galaxy) and a non-thermal (jet) one. But this is not the case for the radio and X-ray bands, where we observe mainly the jet emission. (Though in the X-ray case extended emission from cluster- or group-scale gas can contribute to the observed luminosity.) Therefore, following our results from Section 2, we expect the radio core and X-ray luminosities to increase as the Ca H&K break decreases. Fig. 4 and 5 show that this is indeed the case. The Ca H&K break value is significantly anti-correlated with both the X-ray ( $P > 99.9\%$ ) and radio core luminosity ( $P > 99.9\%$ ). We used the ASURV analysis package (Feigelson & Nelson 1985) in the case of censored data. The

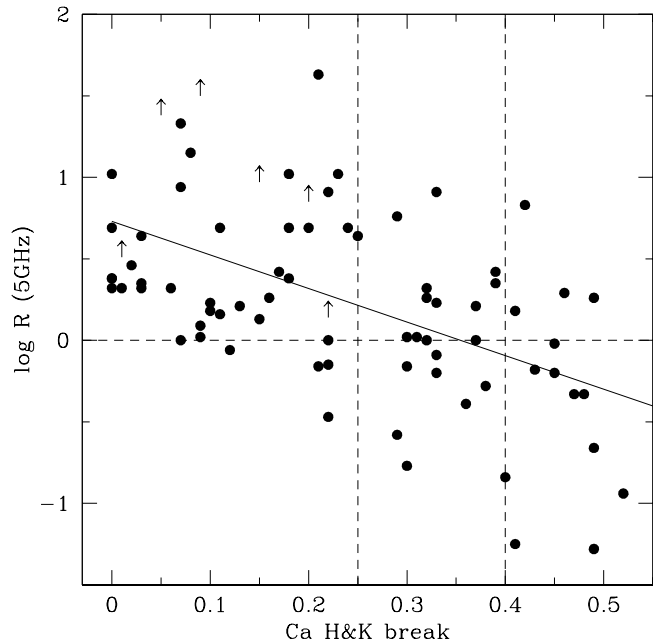


**Figure 6.** The core dominance parameter at 5 GHz vs. the Ca H&K break value. Arrows denote lower limits. The solid line represents the observed correlation. The horizontal dashed line represents the locus of constant  $R = L_{\text{rc}}/L_{\text{ext}} = 1$ . The vertical dashed lines represent Ca H&K break values of  $C = 0.25$  and  $0.4$  suggested by Stocke et al. (1991) and Marchã et al. (1996) respectively to discriminate between BL Lacs and radio galaxies.

correlations remain in both cases very strong ( $P > 99.9\%$ ) even if objects with Ca H&K break values  $C > 0.4$  are excluded, i.e., objects currently defined as radio galaxies. We also verified by means of a partial correlation analysis that all our significant luminosity - Ca H&K break correlations were not induced by a common redshift dependence. In the case of censored data we used the algorithms developed by Akritas & Siebert (1996). Note additionally that, since we made it a requirement for our sources to have information on both radio core and X-ray luminosity, Fig. 4 and 5 include the *same* objects (83 sources).

We find a similarly strong ( $P > 99.9\%$ ) correlation between Ca H&K break value and X-ray luminosity if we consider BL Lacs and radio galaxies from the DXRBS only (21 objects). Note that not all of these sources have a measured radio core luminosity. Additionally, Caccianiga et al. (1999) found a significant correlation between Ca H&K break value and X-ray luminosity for the BL Lacs and radio galaxies from the REX survey, once sources residing in clusters of galaxies were excluded. Since both the DXRBS and REX are homogeneous flux-limited samples, these results suggest that the luminosity - Ca H&K break correlations present in our sample are unlikely to be caused by selection effects.

### 3.2 Intrinsic luminosity range vs. orientation effects

So far we have shown by using observations in the optical, radio and X-ray band that the decrease in Ca H&K break is due to an increase in the object’s jet power. In the following we want to investigate *why* BL Lac objects with a low Ca H&K break have more powerful jets than those with a higher Ca H&K break value. There are two possible explanations: 1. the spread in jet luminosities is intrinsic to the BL Lac class, and/or 2. the spread in jet luminosities (and Ca H&K break value) is induced by orientation effects.

Which of these two possibilities causes the Ca H&K break value to correlate with jet luminosity can be best determined by using information in the radio band. In this range, measurements on both core and extended jet luminosities are available. This is important, since the two powers are affected in a different way by orientation, but similarly if the jet luminosity range is intrinsic. Beaming, i.e., a change in viewing angle, is known to cause only an increase in core luminosity, but not to affect extended power, since the latter is believed to be radiated isotropically. A change in intrinsic luminosity, on the other hand, would be apparent as an increase in both core and extended radio power (e.g., Giovannini et al. 1988) with decreasing Ca H&K break value. For the objects in our sample, no significant ( $P \sim 46\%$ ) correlation is present between Ca H&K break value and extended radio power  $L_{\text{ext}}$ . We note that, though we have limited the extended radio powers of our objects to  $L_{\text{ext}} < 10^{25.6}$  W/Hz, the distributions of both core and extended radio powers have similar dispersions  $\sigma = 0.7$  and  $0.8$  respectively. Therefore, a priori there is no reason why the Ca H&K break value should correlate with radio core but not with extended radio emission.

On the other hand, if the Ca H&K break value can indeed be related to the object’s viewing angle, it is expected to also correlate with the radio core dominance parameter, thought to be a good indicator of orientation. In Fig. 6 we plot for the objects in our sample the radio core dominance parameter at 5 GHz vs. the Ca H&K break value. The former is defined as  $R = L_{\text{rc}}/L_{\text{ext}}$ . A significant ( $P > 99.9\%$ ) linear anti-correlation, albeit with a large scatter, is present between the two quantities. The correlation remains very strong even if we eliminate objects with Ca H&K break values  $C > 0.4$ .

Wolter et al. (2001) presented a plot similar to our Fig. 6 for BL Lacs and FR I radio galaxies from the REX survey. They obtained for their sample ( $\sim 40$  objects) that Ca H&K break value and radio core dominance parameter (at 5 GHz) are only weakly anti-correlated. However, they noted that their radio galaxies were more core-dominated than classical FR Is. In fact, all their objects had radio core dominance parameters  $\log R \geq 0$ . If we include in our analysis only the core-dominated objects, we find that the correlation between Ca H&K break value and radio core dominance parameter also becomes insignificant ( $P = 85\%$ ).

Fig. 6 shows further that the transition between core- and lobe-dominated objects, i.e., between BL Lacs and FR I radio galaxies, seems to occur rather smoothly as the Ca H&K break value (and therefore the viewing angle) changes,

and we find that in the range formerly defined as the BL Lac regime, i.e.,  $0 \leq C \leq 0.25$ , only 11% of the objects are lobe-dominated ( $\log R < 0$ ), whereas this ratio increases in the Ca H&K break value ranges  $0.25 < C \leq 0.4$  and  $C > 0.4$  to 40% and 69% respectively. Therefore, the objects newly included by Marchã et al. (1996) with Ca H&K break values  $0.25 < C \leq 0.4$  seem to represent the long-sought population intermediate between the “classical” BL Lacs and the FR I radio galaxies.

Further support for the assumption that the range in Ca H&K break values represents a range in viewing angles can be found by using the results of Zirbel & Baum (1995) and Hardcastle & Worrall (1999). Zirbel & Baum (1995) obtained for a sample of 81 FR I radio galaxies a mean radio core luminosity of  $23.4 \pm 1.0$  W/Hz. This is consistent with the value of  $\log L_{\text{rc}} = 23.8 \pm 0.3$  W/Hz that the correlation in Fig. 5 gives for  $C = 0.5$ , i.e., for the radio galaxies. Hardcastle & Worrall (1999) could detect in ROSAT pointed observations a core in the X-ray band for 15 of the FR I radio galaxies studied (see their Table 4). For these we obtain a mean ROSAT X-ray core luminosity  $\log L_{\text{x}} = 17.2 \pm 0.9$  W/Hz. This is in good agreement with the value of  $\log L_{\text{x}} = 17.6 \pm 0.5$  W/Hz that the correlation in Fig. 4 gives for  $C = 0.5$ . Therefore, our luminosity - Ca H&K break correlations which we obtained including both BL Lacs and FR I radio galaxies seem to reproduce well the average radio and X-ray luminosities of (rather large samples of) FR I radio galaxies.

## 4 THE RELATION BETWEEN CA H&K BREAK VALUE AND VIEWING ANGLE

### 4.1 Luminosity ratios and viewing angle

We now want to investigate how the Ca H&K break value might be used to constrain the viewing angle. We have then simulated for the radio and X-ray band the expected luminosity ratio between the BL Lac object and the parent radio galaxy as the viewing angle  $\phi_{\text{GAL}}$  changes. We used the formula given in Capetti & Celotti (1999):

$$L_{\text{BL}}/L_{\text{GAL}} = [(1 - \beta \cdot \cos\phi_{\text{GAL}})/(1 - \beta \cdot \cos\phi_{\text{BL}})]^{(p+\alpha)},$$

where  $\beta$  is the bulk velocity in units of the speed of light, and  $\phi$  is the angle between the velocity vector and the line of sight. We chose the case of a continuous jet ( $p = 2$ ). For the simulations in the radio band we assumed a radio spectral index  $\alpha_{\text{r}} = 0.2$ , corresponding to the mean value for the objects in our sample, while for the X-ray band we chose  $\alpha_{\text{x}} = 1.4$ , following the results of Padovani & Giommi (1996). The simulations were performed assuming the three cases  $\phi_{\text{BL}} = 0^\circ, 10^\circ, \text{ and } 20^\circ$ , and a changing  $\phi_{\text{GAL}}$  up to a maximum value of  $90^\circ$ . In our case, the quantity  $\phi_{\text{BL}}$  is fixed and represents the angle below which the jet/galaxy ratio is so high that the Ca H&K break value is constant and equal to zero. Only  $\phi_{\text{GAL}}$  is assumed to change as the Ca H&K break value increases. For each case of  $\phi_{\text{BL}}$  we assumed jet Lorentz factors  $\Gamma = 1/\sqrt{1 - \beta^2} = 2, 3$  and  $4$ . Our results for the radio and X-ray band are shown in Fig.



**Table 2.** Approximate average viewing angles of FR I galaxies

BL Lac angle:	0°	10°	20°
$\Gamma = 4$	32°	40°	58°
$\Gamma = 3$	44°	50°	66°
$\Gamma = 2$	72°	77°	> 90°

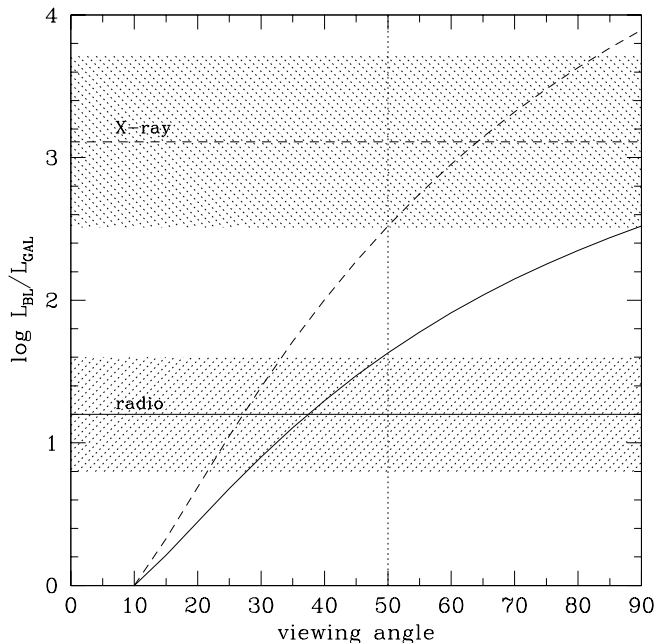


**Figure 7.** Simulated  $L_{\text{BL}}/L_{\text{GAL}}$  ratios in the X-ray (dashed line) and radio band (solid line) for a Lorentz factor  $\Gamma = 3$ , assuming a fixed BL Lac viewing angle  $\phi_{\text{BL}} = 10^\circ$  and a changing FR I galaxy viewing angle  $\phi_{\text{GAL}}$  (see text for details). Horizontal lines indicate the ratios inferred from Fig. 4 and 5 in the X-ray (dashed line) and radio band (solid line) respectively. The  $2\sigma$  error on the ratios is shown by the shaded areas. The vertical dotted line represents the FR I galaxy viewing angle at which the observed  $L_{\text{BL}}/L_{\text{GAL}}$  ratios in the radio and X-ray band are reproduced approximately simultaneously.

7, representatively for the case of  $\phi_{\text{BL}} = 10^\circ$  and Lorentz factor  $\Gamma = 3$ .

From the best fits in Fig. 4 and 5 we get a maximum ratio of  $\log L_{\text{BL}}/L_{\text{GAL}} = 3.11 \pm 0.30$  and  $1.20 \pm 0.20$  for the X-ray and radio band respectively, where  $L_{\text{BL}}$  is the luminosity at the Ca H&K break value  $C = 0$  and  $L_{\text{GAL}}$  the luminosity at  $C = 0.5$ . Our simulations show that in all three cases assumed for  $\phi_{\text{BL}}$  and  $\Gamma$  it is possible to reproduce these two ratios within their  $2\sigma$  errors simultaneously, i.e., with the same Lorentz factor and approximately with the same maximum viewing angle. Our results are listed in Table 2. The derived viewing angles represent the angles under which we expect to observe on average an FR I radio galaxy with a Ca H&K break value of  $C = 0.5$ . These are not to be confused with maximum viewing angles for FR I radio galaxies, which can be larger, or with the critical viewing

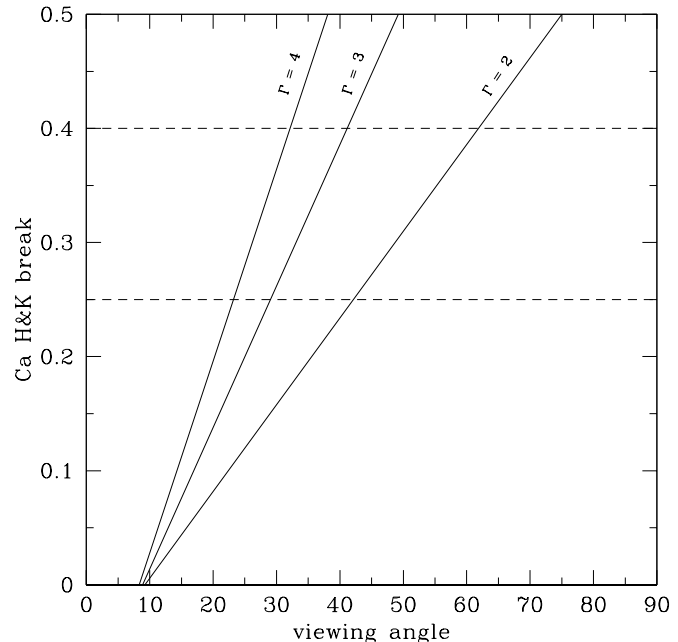


**Figure 8.** The correlation Ca H&K break value vs. viewing angle for a starting viewing angle  $\phi_{\text{BL}} = 10^\circ$  and Lorentz factors  $\Gamma = 2, 3$  and 4 as obtained from connecting the correlations in Fig. 4 and 5 with our simulations exemplified in Fig. 7.

angle, i.e., the angle separating BL Lacs from FR I radio galaxies. From Table 2 we see that the case of a starting BL Lac viewing angle  $\phi_{\text{BL}} = 20^\circ$  and a Lorentz factor  $\Gamma = 2$  is unphysical, since it gives typical viewing angles for radio galaxies above  $90^\circ$ . Higher Lorentz factors than the ones simulated here would result in smaller angles for the radio galaxies. Similarly for the case of  $p = 3$ , describing a moving, isotropic source.

Our resulting viewing angles and Lorentz factors for FR I radio galaxies agree with values obtained using independent methods, validating our use of the Ca H&K break value as an orientation indicator. Giovannini et al. (2001) constrained the Lorentz factor for parsec-scale jets in both low- and high-power radio galaxies to  $\Gamma = 3 - 10$  based on the scatter of their correlation between core and total radio power. Urry & Padovani (1995) obtained from luminosity function studies of BL Lacs and FR I radio galaxies average Lorentz factors of  $\Gamma = 3 - 7$  and critical angles  $\phi_c = 12 - 30^\circ$ . The latter transform to average viewing angles for the FR Is in the range  $58 - 63^\circ$  if we use their equation (A12). Chiberge et al. (2000) derived from the observed differences in core power between BL Lacs and FR Is with similar extended radio powers average Lorentz factors  $\Gamma \sim 5$ , if maximum viewing angles  $\phi = 1/\Gamma$  and  $60^\circ$  are assumed for BL Lacs and FR Is respectively. Verdoes Kleijn et al. (2002) used the correlation between radio core and  $\text{H}\alpha + [\text{NII}]$  core emission for their sample of FR I radio galaxies and constrained the average Lorentz factors to  $\Gamma \sim 2 - 5$ , assuming viewing angles in the range  $\phi = [30^\circ, 90^\circ]$ .

#### 4.2 Ca H&K break value and viewing angle

We want now to investigate how the Ca H&K break value can be converted to viewing angle. For this purpose, we determine from the correlations in Fig. 4 and 5 for a range of Ca H&K break values the ratio  $L_{\text{BL}}/L_{\text{C}}$  in the X-ray and radio band. We assume  $L_{\text{BL}}$  to be the luminosity at the Ca H&K break value  $C = 0$ , and define  $L_{\text{C}}$  as the luminosity at  $C = 0.1, 0.2, 0.3, 0.4$  and  $0.5$ . We then convert the  $L_{\text{BL}}/L_{\text{C}}$  ratios observed in the two bands to a viewing angle using our simulations exemplified in Fig. 7. Since each  $L_{\text{BL}}/L_{\text{C}}$  ratio pair also corresponds to an individual Ca H&K break value, we obtain in this way a correlation between Ca H&K break and viewing angle. The linear fits to the data points are shown in Fig. 8 for a jet of Lorentz factor  $\Gamma = 2, 3$  and  $4$ , and assuming for  $C = 0$  a starting viewing angle of  $\phi_{\text{BL}} = 10^\circ$ .

From Fig. 8, we see that by extending the “classical” Ca H&K break value of  $0.25$  to  $0.4$  as proposed by Marchã et al. (1996), BL Lac surveys include sources seen at larger viewing angles, and therefore less beamed. This is supported by the recent results of Dennett-Thorpe & Marchã (2000), who find that BL Lac objects with  $C > 0.25$ , the so-called BL Lac candidates, are significantly less polarized at  $8.4$  GHz than BL Lacs with  $C < 0.25$ .

#### 5 LOW- AND HIGH-ENERGY PEAKED BL LACS

The BL Lac class is currently divided into two subclasses: low- (LBL) and high-energy peaked BL Lacs (HBL), i.e., objects with a synchrotron emission peak located in the IR/optical and UV/soft X-ray band respectively. This division was introduced by Padovani & Giommi (1995) after it was first discovered that BL Lacs detected in radio (RBL) and X-ray surveys (XBL) had different radio-to-X-ray flux ratios, and that this was due to the fact that their spectral energy distributions (SED) had different shapes (Giommi, Ansari & Micol 1995).

As of today the question of how the two BL Lac subclasses are connected with each other regarding, e.g., their physical properties or evolutionary behaviour, is a matter of fervent debate. A finding that shaped strongly our perception of BL Lacs was made by Maraschi et al. (1986). These authors found that radio- and X-ray-selected blazars differed considerably in their radio luminosities, but had similar X-ray powers. Based on this, they concluded that the X-ray radiation was less beamed than the radio one, and that HBL being radio-weak were objects viewed at larger angles than LBL. However, Sambruna, Maraschi & Urry (1996) later showed that the typical SED of an XBL cannot be obtained from the SED of an RBL simply by changing the viewing angle alone.

If we divide the objects in our sample into LBL (defined by  $\log L_{\text{rc}}/L_{\text{x}} \geq 6$  [Padovani & Giommi 1996]; 18 objects) and HBL (defined by  $\log L_{\text{rc}}/L_{\text{x}} < 6$ ; 65 objects), we find similarly to the entire sample that their X-ray and radio core luminosities are strongly anti-correlated with Ca H&K break value (Fig. 9 and 10 respectively). Note that we subdivided

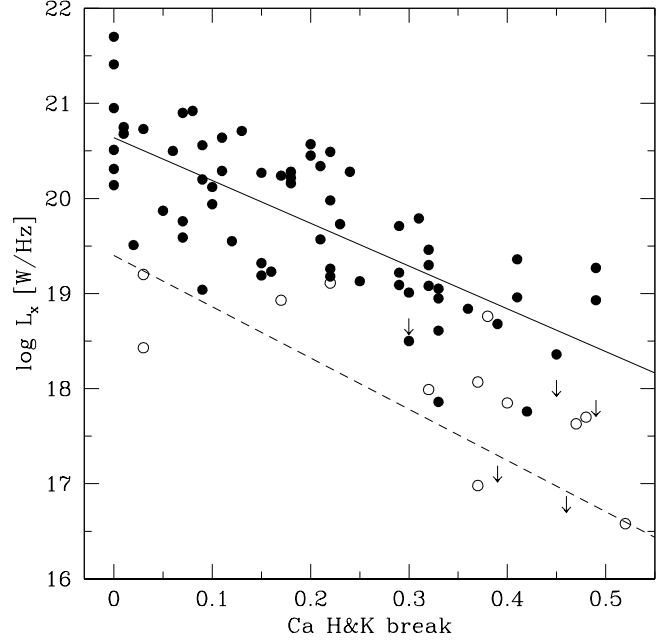


**Figure 9.** The 1 keV X-ray luminosity vs. the Ca H&K break value. Open and filled circles denote LBL ( $\log L_{\text{rc}}/L_{\text{x}} \geq 6$ ) and HBL ( $\log L_{\text{rc}}/L_{\text{x}} < 6$ ) respectively. Arrows indicate LBL with upper limits on the X-ray luminosity. Solid and dashed lines represent the observed correlations for HBL and LBL respectively. Object 1241+735 is off the plot.

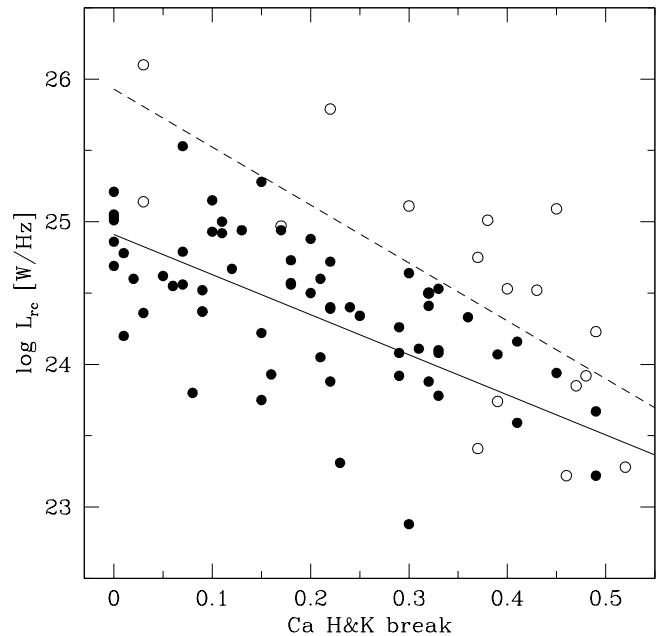


**Figure 10.** The radio core luminosity at 5 GHz vs. the Ca H&K break value. Open and filled circles denote LBL ( $\log L_{\text{rc}}/L_{\text{x}} \geq 6$ ) and HBL ( $\log L_{\text{rc}}/L_{\text{x}} < 6$ ) respectively. Solid and dashed lines represent the observed correlations for HBL and LBL respectively.

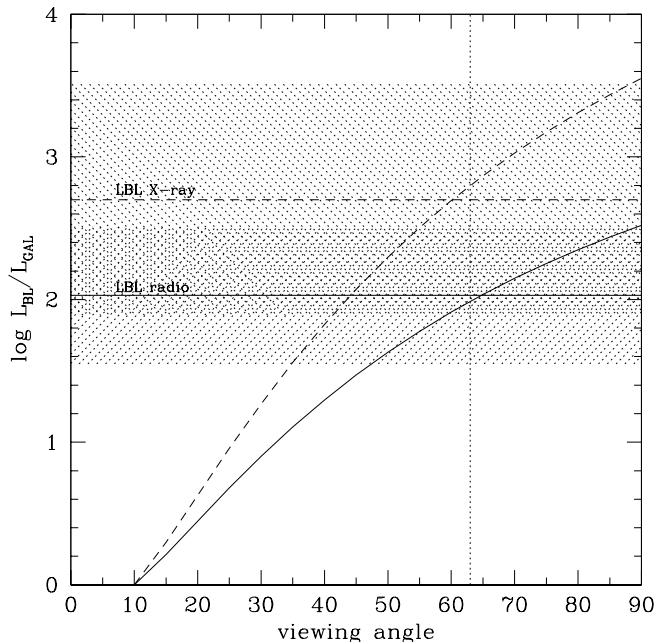


**Figure 11.** Simulated  $L_{\text{BL}}/L_{\text{GAL}}$  ratios for LBL in the X-ray (dashed line) and radio band (solid line) for a changing viewing angle and a Lorentz factor  $\Gamma = 3$ . Horizontal lines indicate the ratios inferred from Fig. 9 and 10 in the X-ray (dashed line) and radio band (solid line) respectively. The  $1\sigma$  error on the ratios is shown by the shaded areas. The vertical dotted line represents the viewing angle at which the observed  $L_{\text{BL}}/L_{\text{GAL}}$  ratios for LBL in the radio and X-ray band are reproduced approximately simultaneously.

all the objects in our sample, i.e., independent of Ca H&K break value. We think that this approach is justified since we are using the radio core instead of the total radio power to define LBL and HBL. The significance level is  $P > 99.9\%$  for all four correlations. This finding allows us, on one hand, to derive typical viewing angles for LBL and HBL, and, on the other hand, to compare the luminosities of the two BL Lac subclasses at different orientations.

### 5.1 Viewing angles

We performed the simulations described in Sect. 4.1 individually for the two BL Lac subclasses.

The LBL and HBL in our sample have mean radio spectral indices  $\alpha_r = 0.1 \pm 0.1$  and  $0.3 \pm 0.1$  respectively, not significantly different ( $P = 93.7\%$ ) according to a Student's t-test. Therefore, we assumed for the simulations in the radio band for both LBL and HBL a radio spectral index  $\alpha_r = 0.2$ . On the other hand, the X-ray spectral index is known to be different for the two types of BL Lacs. Therefore, we performed the simulations in the X-ray band independently for LBL and HBL and used, following the results of Padovani & Giommi (1996),  $\alpha_x = 1.1$  and  $1.5$  respectively.

From the best fits in Fig. 9 and 10 we get for LBL a maximum ratio of  $\log L_{\text{BL}}/L_{\text{GAL}} = 2.70 \pm 0.81$  and  $2.03 \pm$

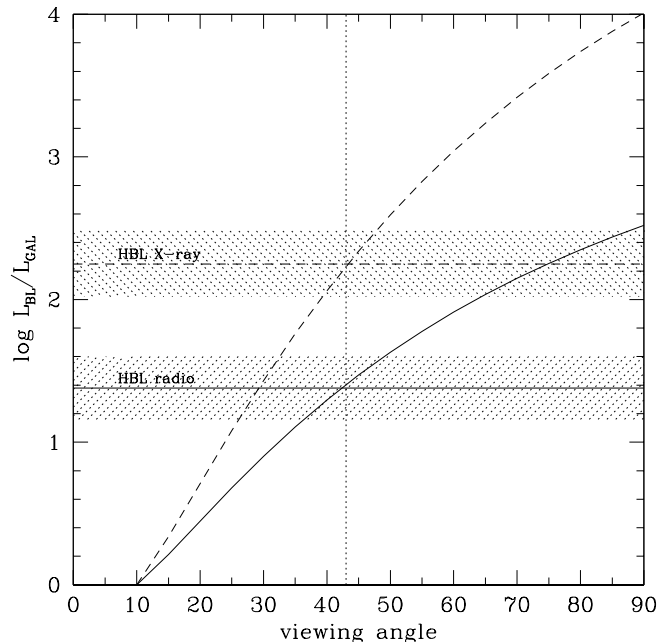


**Figure 12.** Simulated  $L_{\text{BL}}/L_{\text{GAL}}$  ratios for HBL in the X-ray (dashed line) and radio band (solid line) for a changing viewing angle and a Lorentz factor  $\Gamma = 3$ . Horizontal lines indicate the ratios inferred from Fig. 9 and 10 in the X-ray (dashed line) and radio band (solid line) respectively. The  $1\sigma$  error on the ratios is shown by the shaded areas. The vertical dotted line represents the viewing angle at which the observed  $L_{\text{BL}}/L_{\text{GAL}}$  ratios for HBL in the radio and X-ray band are reproduced approximately simultaneously.

0.48 for the X-ray and radio band respectively, where  $L_{\text{BL}}$  is the luminosity at the Ca H&K break value  $C = 0$  and  $L_{\text{GAL}}$  the luminosity at  $C = 0.5$ . For HBL, we obtain from the best fits in Fig. 9 and 10 ratios  $\log L_{\text{BL}}/L_{\text{GAL}} = 2.25 \pm 0.26$  and  $1.38 \pm 0.22$  for the X-ray and radio band respectively.

Our simulations show that in all cases assumed for  $\phi_{\text{BL}}$  and  $\Gamma$  (see Sect. 4.1) it is possible to reproduce the ratios in the radio and X-ray band for both LBL (Fig. 11) and HBL (Fig. 12) simultaneously, i.e., with the same Lorentz factor and the same maximum viewing angle. The viewing angles that we obtain in this way are similar to the ones listed in Table 2. We note that in the case of LBL we get somewhat higher viewing angles than for HBL. However, this difference is not significant ( $P = 77.0\%$ ). A significantly larger range in viewing angles would imply that LBL were more beamed than HBL. This becomes clear if one recalls that in our simulations we assumed the same Lorentz factor for LBL and HBL. Alternatively, we could have fixed the range in viewing angles, which would have resulted in larger Lorentz factors for LBL.

### 5.2 Radio and X-ray luminosity differences

Our use of the Ca H&K break value allows us to evaluate and compare for the first time the radio and X-ray luminosities of

**Table 4.** Mean radio core and X-ray luminosities\* of LBL and HBL

	FR I HBL	FR I LBL	$P$	FR I&II LBL	$P$	FR II LBL	$P$
$\log L_x$	$19.77 \pm 0.10$	$17.49 \pm 0.34$	$> 99.9\%$	$18.04 \pm 0.36$	$> 99.9\%$	$19.71 \pm 0.50$	8.0%
$\log L_{rc}$	$24.36 \pm 0.08$	$24.51 \pm 0.19$	57.9%	$25.14 \pm 0.26$	99.3%	$26.77 \pm 0.25$	$> 99.9\%$
$z$	$0.21 \pm 0.02$	$0.10 \pm 0.02$	$> 99.9\%$	$0.23 \pm 0.05$	37.3%	$0.57 \pm 0.07$	$> 99.9\%$

\* luminosities in units of [W/Hz]

**Table 3.** Radio core and X-ray luminosities\* of LBL and HBL derived from correlations in Fig. 9 and 10

		LBL	HBL	$P$
$C = 0$	$\log L_x$	$19.40 \pm 0.59$	$20.65 \pm 0.12$	96.4%
	$\log L_{rc}$	$25.93 \pm 0.36$	$24.90 \pm 0.11$	98.8%
$C = 0.5$	$\log L_x$	$16.71 \pm 1.00$	$18.39 \pm 0.28$	89.0%
	$\log L_{rc}$	$23.90 \pm 0.60$	$23.51 \pm 0.25$	45.1%

\* luminosities in units of [W/Hz]

LBL and HBL at different orientations. In Table 3 we list the X-ray and radio core powers resulting from the correlations in Fig. 9 and 10 for LBL and HBL at small ( $C = 0$ ) and large ( $C = 0.5$ ) Ca H&K break values and therefore viewing angles. From this we get that at large viewing angles LBL and HBL have similar radio core and X-ray powers, i.e., they reside in FR I radio galaxies with similar properties (radio core and X-ray luminosities), while at relatively small viewing angles the two BL Lac subclasses differ significantly in their luminosities. In this case we get that LBL are  $\approx 10$  times more luminous in the radio and by a similar factor less luminous in the X-ray band than HBL. We stress that the objects used in this work form an heterogeneous sample of sources from different surveys with widely different flux limits. Therefore, although we believe that these luminosity differences are present, their precise values might depend on the selected objects. In the following we want to expand on the influence of selection effects on the luminosity differences between LBL and HBL.

For this purpose we have also included BL Lacs with extended radio powers more typical of FR II radio galaxies ( $L_{\text{ext}} > 10^{25.6}$  W/Hz). Furthermore, we distinguished between the following three cases: 1. a comparison between HBL (65 objects) and LBL (18 objects), where both have extended radio emissions typical of FR I radio galaxies; 2. a comparison between HBL (65 objects) and LBL (25 objects), where the latter are selected independent of extended radio emission; 3. a comparison between HBL (65 objects) and LBL (7 objects), where the latter have extended radio emissions typical of FR II radio galaxies. The most important difference between these three cases is that we compare HBL and LBL that are first matched and then not matched in extended radio power, i.e., have a similar parent population.

For the three cases, we obtain the following results, illustrated in Table 4:

1. In the first case, where we compare LBL and HBL with similar extended radio powers, we get that they have similar mean radio core luminosities, while HBL have higher

mean X-ray luminosities than LBL. In this case, we get that LBL have a significantly lower mean redshift than HBL.

2. In the second case, where we compare LBL and HBL with somewhat different extended radio powers, we get that LBL have higher mean radio core luminosities and lower mean X-ray luminosities than HBL. In this case, LBL and HBL have similar mean redshifts.

3. In the third case, where we compare LBL with high extended radio powers and HBL with low extended radio powers, we get that the two BL Lac subclasses have similar mean X-ray luminosities, while LBL have higher mean radio core luminosities than HBL. In this case, LBL have a significantly higher mean redshift than HBL.

These comparisons show that the resulting luminosity differences between LBL and HBL seem to depend strongly on the samples chosen. In particular, our three cases illustrate that, the more LBL and HBL differ in their extended radio powers, the less they differ in their X-ray powers. We note that these luminosity differences cannot be due only to a redshift effect. If that were the case, in fact, higher-redshift samples would be more luminous in all bands, contrary to what observed.

We can further illustrate these selection effects by using two different samples: the sample of Maraschi et al. (1986) that contains LBL and HBL with similar X-ray powers, and the complete sample of BL Lacs from the DXRBS which is radio-flux limited and therefore contains LBL and HBL with similar radio powers. Nearly half of the objects in the sample used by Maraschi et al. (1986) are strong-lined objects, i.e., radio quasars. Therefore, in order to compare their results with ours we selected from their sample only the BL Lac objects. Similarly to their results for radio- and X-ray-selected blazars, we get that their LBL (17 objects) and HBL (11 objects) have similar mean X-ray powers, but significantly different ( $P > 99.9\%$ ) mean (total) radio luminosities  $\log L_r = 26.61 \pm 0.25$  and  $24.56 \pm 0.08$  W/Hz respectively. The mean redshifts are  $z = 0.35 \pm 0.08$  and  $0.12 \pm 0.03$  for LBL and HBL respectively, different at the 98.8% level. This result is similar to our case 3, indicating that these authors have compared radio-strong LBL with radio-weak HBL.

For the sample of DXRBS BL Lacs, we get that LBL (20 objects) and HBL (12 objects) have similar mean radio powers, but significantly different ( $P = 98.7\%$ ) mean X-ray powers  $\log L_x = 18.98 \pm 0.23$  and  $20.00 \pm 0.32$  W/Hz respectively. In this case LBL and HBL have similar mean redshifts. This result shows that our first case can be reproduced with a radio-flux limited sample.

Now the question arises: ‘‘Which is the best approach to clarify what are the intrinsic luminosity differences between LBL and HBL in a given band?’’. We think that this can be answered in a physically meaningful way by comparing

LBL and HBL with a similar parent population, i.e., with similar extended radio powers. Ideally, if information on the Ca H&K break value is available, one should also take into account orientation effects by separating sources according to viewing angle.

## 6 DISCUSSION AND CONCLUSIONS

We have suggested that the Ca H&K break value of BL Lacs and FR I radio galaxies is a direct indicator of viewing angle. We have based this on the strong anti-correlation between Ca H&K break value and optical, radio, X-ray jet luminosity, and radio core dominance parameter. We have excluded the possibility that the observed range in radio jet power is intrinsic and not due to orientation, since we could not find a similarly strong correlation between Ca H&K break value and extended radio emission for our sample of objects.

Stocke et al. (1991) introduced a limit of 25% on the allowed Ca H&K break value for BL Lacs, which was later expanded by Marchã et al. (1996) up to a value of 40%, in connection with the strength of observed emission lines. Our result implies that those BL Lacs with Ca H&K break values  $0.25 \leq C \leq 0.4$ , termed by Marchã et al. (1996) “BL Lac candidates”, represent in fact the long-sought population of objects with viewing angles intermediate between the “classical” BL Lacs and FR I radio galaxies.

Which limit on the Ca H&K break value should be chosen to separate BL Lacs from FR I radio galaxies? In general, BL Lacs are those objects viewed at angles smaller than a certain critical angle, which has been defined in the literature as the angle for which the radio core dominance parameter is equal to 1 (Urry & Padovani 1995). From the correlation between the radio core dominance parameter and Ca H&K break value illustrated in Fig. 6 we infer that a Ca H&K break value  $\sim 0.35$  would then be appropriate to separate BL Lacs (core-dominated) from radio galaxies (lobe-dominated). We note that this value is very close to 0.4, proposed by Marchã et al. (1996).

We have shown that the Ca H&K break value is a suitable indicator of orientation. So far, only one other such indicator was known: the radio core dominance parameter. However, the determination of this quantity usually requires dedicated radio observations, which are time consuming and not always available. Therefore, our result that we can constrain the viewing angle of a BL Lac or FR I radio galaxy from such a common astrophysical observation as its optical spectrum will be a considerable advantage in our studies of unified schemes.

We have shown for our full sample that radio and X-ray jets of BL Lacs and FR I radio galaxies have similar Lorentz factors and are viewed under similar angles, namely the radio and X-ray Doppler factors are the same (within the errors). This result becomes even more significant if we separate our sample into low- (LBL) and high-energy peaked BL Lacs (HBL).

We have also shown that LBL and HBL have jets with similar Lorentz factors, viewed under similar angles, i.e., their Doppler factors are similar. This result is in agreement with the “different peak energy” scenario (Padovani

& Giommi 1995), which claims that the only difference between LBL and HBL is the frequency position of their synchrotron emission peak. However, we note that there is a hint in our data that LBL might be more beamed than HBL, i.e., they might have either larger Lorentz factors or span a larger range in viewing angles. But given that our sample is heterogeneous, this might be induced by selection effects.

Our finding that the Ca H&K break value is directly related to viewing angle has allowed us to compare for the first time the luminosities of the two types of BL Lacs at different orientations. We derive that FR I radio galaxies harbouring LBL and HBL have similar radio core and X-ray luminosities. At small viewing angles, LBL have radio cores  $\approx 10$  times more powerful than HBL ones, while the opposite is true in the X-ray band. These two results combined appear to be at odds with our previous result that LBL and HBL have similar Doppler factors. We attribute this apparent contradiction to small number statistics. Note in fact that HBL-like and LBL-like FR Is also differ in their powers in the same sense as HBL and LBL but their differences are not significant due to the larger errors at  $C \sim 0.5$ .

We have also discussed the issue of selection effects on the study of luminosity differences between HBL and LBL, and have shown that the comparison to be meaningful has to be done for samples with similar parent populations, i.e., similar extended radio powers.

To summarize, we have reached the following conclusions:

- (i) The value of the Ca H&K break in BL Lacs and FR I radio galaxies decreases with increasing jet power.
- (ii) The increase in jet power is caused by a change in viewing angle.
- (iii) BL Lacs with Ca H&K break values  $0.25 \leq C \leq 0.4$ , termed by Marchã et al. (1996) “BL Lac candidates”, are the long-sought population with viewing angles intermediate between the “classical” BL Lacs and FR I radio galaxies.
- (iv) BL Lacs and FR I radio galaxies have radio and X-ray jets with similar Lorentz factors ( $\sim 2 - 4$ ), and viewed under similar angles, i.e., their jets have similar radio and X-ray Doppler factors.
- (v) The two types of BL Lacs, LBL and HBL, have jets with similar Lorentz factors, which are viewed under similar angles, i.e., they are affected by beaming in a similar way.
- (vi) LBL and HBL reside in FR I radio galaxies with similar radio core and X-ray powers. However, at small viewing angles, LBL have radio cores  $\approx 10$  times more powerful than HBL ones, while the opposite is true in the X-ray band.

In future work we plan to investigate the emission line properties of BL Lacs in order to understand in what way they are related to their more powerful siblings, the flat spectrum radio quasars. With this we hope to be able to give a more complete picture of what a BL Lac really is.

## ACKNOWLEDGEMENTS

We would like to thank Eric Perlman, Manfred Stickel, and Clive Tadhunter for providing several spectra in electronic format. H.L. acknowledges financial support from the

Deutscher Akademischer Austauschdienst (DAAD) and the STScI DDRF grant D0001.82260.

## REFERENCES

- Akritas, M. G., Siebert, J., 1996, *MNRAS*, 278, 919
- Augusto P., Wilkinson P. N., Browne I. W. A., 1998, *MNRAS*, 299, 1159
- Bade N., Beckmann V., Douglas N. G., Barthel P. D., et al., 1998, *A&A*, 334, 459
- Blandford R. D., Rees M. J., 1978, in *Pittsburgh Conference on BL Lac Objects*, ed. A. M. Wolfe, p. 328
- Bondi M., Marchã M. J. M., Dallacasa D., Stanghellini C., 2001, *MNRAS*, 325, 1109
- Brinkmann W., Siebert J., Boller T., 1994, *A&A*, 281, 355
- Brinkmann W., Siebert J., Reich W., Fürst E., et al., 1995, *A&AS*, 109, 147
- Brinkmann W., Siebert J., Feigelson E. D., Kollgaard R. I., et al., 1997, *A&A*, 323, 739
- Browne I. W. A., Marchã M. J. M., 1993, *MNRAS*, 261, 795
- Bruzual A. G., 1983, *ApJ*, 273, 105
- Caccianiga A., Maccacaro T., Wolter A., Della Ceca R., Gioia I. M., 1999, *ApJ*, 513, 51
- Caccianiga A., Maccacaro T., Wolter A., Della Ceca R., Gioia I. M., 2000, *A&AS*, 144, 247
- Capetti A., Celotti A., 1999, *MNRAS*, 304, 434
- Cassaro P., Stanghellini C., Bondi M., Dallacasa D., et al., 1999, *A&AS*, 139, 601
- Chiaberge M., Celotti A., Capetti A., Ghisellini G., 2000, *A&A*, 358, 104
- Dennett-Thorpe J., Marchã M. J., 2000, *A&A*, 361, 480
- Dressler A., Shectman S. A., 1987, *AJ*, 94, 899
- Falomo R., Scarpa R., Bersanelli M., 1994, *ApJS*, 93, 125
- Fanaroff B. L., Riley J. M., 1974, *MNRAS*, 167, 31
- Feigelson E. D., Nelson P. I., 1985, *ApJ*, 293, 192
- Giommi P., Ansari S. G., Micol A., 1995, *A&AS*, 109, 267
- Giommi P., Menna M. T., Padovani P., 1999, *MNRAS*, 310, 465
- Giovannini G., Feretti L., Gregorini L., Parma P., 1988, *A&A*, 199, 73
- Giovannini G., Cotton W. D., Feretti L., Lara L., Venturi T., 2001, *ApJ*, 552, 508
- Gregory P. C., Scott W. K., Douglas K., Condon J. J., 1996, *ApJS*, 103, 427
- Griffith M. R., Wright A. E., 1993, *AJ*, 105, 1666
- Hardcastle M. J., Worrall D. M., 1999, *MNRAS*, 309, 969
- Heidt J., Wagner S. J., 1996, *A&A*, 305, 42
- Heidt J., Wagner S. J., 1998, *A&A*, 329, 853
- Jannuzi B. T., Smith P. S., Elston R., 1994, *ApJ*, 428, 130
- Kühr H., Schmidt G. D., 1990, *AJ*, 99, 1
- Landt H., Padovani P., Perlman E. S., Giommi P., et al., 2001, *MNRAS*, 323, 757
- Laurent-Muehleisen S. A., Kollgaard R. I., Ryan P. J., Feigelson E. D., et al., 1997, *A&AS*, 122, 235
- Laurent-Muehleisen S. A., Kollgaard R. I., Ciardullo R., Feigelson E. D., et al., 1998, *ApJS*, 118, 127
- Laurent-Muehleisen S. A., Kollgaard R. I., Feigelson E. D., Brinkmann W., Siebert J., 1999, *ApJ*, 525, 127
- Maraschi L., Ghisellini G., Tanzi E. G., Treves A., 1986, *ApJ*, 310, 325
- Marchã M. J. M., Browne I. W. A., Impey C. D., Smith P. S., 1996, *MNRAS*, 281, 425
- Morganti R., Killeen N. E. B., Tadhunter C. N., 1993, *MNRAS*, 263, 1023
- Morris S. L., Stocke J. T., Gioia I. M., Schild R. E., et al., 1991, *ApJ*, 380, 49
- Murphy D. W., Browne I. W. A., Perley R. A., 1993, *MN*, 264, 298
- Nass P., Bade N., Kollgaard R. I., Laurent-Muehleisen S. A., et al., 1996, *A&A*, 309, 419
- Owen F. N., Ledlow M. J., 1994, in *The First Stromlo Symposium: The Physics of Active Galaxies*, ed. Bicknell G. V., Dopita M. A., Quinn P. J., p. 319
- Owen F. N., Ledlow M. J., Keel W. C., 1996, *AJ*, 111, 53
- Padovani P., Giommi P., 1995, *ApJ*, 444, 567
- Padovani P., Giommi P., 1996, *MNRAS*, 279, 526
- Perlman E. S., Stocke J. T., 1993, *ApJ*, 406, 430
- Perlman E. S., Stocke J. T., Wang Q. D., Morris S. L., 1996a, *ApJ*, 456, 451
- Perlman E. S., Stocke J. T., Schachter J. F., Elvis M., et al., 1996b, *ApJS*, 104, 251
- Perlman E. S., Padovani P., Giommi P., Sambruna R., et al., 1998, *AJ*, 115, 1253
- Rector T. A., Stocke J. T., Perlman E. S., 1999, *ApJ*, 516, 145
- Rector T. A., Stocke J. T., Perlman E. S., Morris S. L., Gioia I. M., 2000, *AJ*, 120, 1626
- Rector T. A., Stocke J. T., 2001, *AJ*, 122, 565
- Sambruna R. M., Maraschi L., Urry C. M., 1996, *ApJ*, 463, 444
- Siebert J., Brinkmann W., Drinkwater M. J., Yuan W., et al., 1998, *MNRAS*, 301, 261
- Stickel M., Padovani P., Urry C. M., Fried J. W., Kühr H., 1991, *ApJ*, 374, 431
- Stickel M., Meisenheimer K., Kühr H., 1994, *A&AS*, 105, 211
- Stocke J. T., Morris S. L., Gioia I. M., Maccacaro T., et al., 1991, *ApJS*, 76, 813
- Tadhunter C. N., Morganti R., di Serego-Alighieri S., Fosbury R. A. E., Danziger I. J., 1993, *MNRAS*, 263, 999
- Taylor G. B., Vermeulen R. C., Readhead A. C. S., Pearson T. J., et al., 1996, *ApJS*, 107, 37
- Urry C. M., Padovani P., 1995, *PASP*, 107, 803
- Urry C. M., Scarpa R., O'Dowd M., Falomo R., et al., 2000, *ApJ*, 532, 816
- Verdoes Kleijn, G. A., Baum, S. A., de Zeeuw, P. T., O'Dea, C. P., 2002, *AJ*, in press
- Voges W., Aschenbach B., Boller T., Bräuninger H., et al., 1999, *A&A*, 349, 389
- Wall J. V., Peacock J. A., 1985, *MNRAS*, 216, 173
- Wolter A., Caccianiga A., Maccacaro T., et al., 2001, in *Blazar Demographics and Physics*, eds. Padovani P., Urry C. M., p. 190
- Wurtz R., Stocke J. T., Yee H. K. C., 1996, *ApJS*, 103, 109
- Zirbel E. L., Baum S. A., 1995, *ApJ*, 448, 521